

New Reduced Ternary Titanates from Borate Fluxes

B. HESSEN, S. A. SUNSHINE, AND T. SIEGRIST

*AT&T Bell Laboratories, 600 Mountain Avenue,
Murray Hill, New Jersey 07974*

Received March 4, 1991; in revised form May 31, 1991

Single crystals of the new reduced strontium titanate $\text{SrTi}_{11}\text{O}_{20}$ (space group $P\bar{1}$, $a = 7.1252(8) \text{ \AA}$, $b = 7.6644(8) \text{ \AA}$, $c = 13.1577(16) \text{ \AA}$, $\alpha = 90.21(1)^\circ$, $\beta = 92.79(1)^\circ$, $\gamma = 103.94(1)^\circ$) are formed by slowly cooling $\text{SrTiO}_{2.5}$ in molten $\text{SrO} \cdot 2\text{B}_2\text{O}_3$ flux in high vacuum. The compound crystallizes in a new structure type based on sheared double and single rutile chains of TiO_6 octahedra. Formation of a new monoclinically distorted reduced Ti-hollandite, $\text{La}_{1.33}\text{Ti}_8\text{O}_{16}$ (space group $I2/m$, $a = 9.946(2) \text{ \AA}$, $b = 2.9668(4) \text{ \AA}$, $c = 10.280(2) \text{ \AA}$, $\beta = 91.09(2)^\circ$), was observed upon dissolving LaTiO_3 in a molten $\text{La}_2\text{O}_3 \cdot 3\text{B}_2\text{O}_3$ flux. The crystal structures of both compounds were determined by single crystal X-ray diffraction. © 1991 Academic Press, Inc.

Introduction

The reduced ternary oxides of titanium form a class of compounds that can exhibit interesting electronic properties as well as intriguing structural features. Some species are superconductors, such as SrTiO_{3-x} (1, 2) and the spinel $\text{Li}_{1+x}\text{Ti}_{2-x}\text{O}_4$ for $x < 0.16$ (3, 4). Often, complex ternary titanates adopt structures based on sheared chains of TiO_6 octahedra as in $\text{Na}_2\text{Ti}_6\text{O}_{13}$ (5), $\text{Na}_2\text{Ti}_7\text{O}_{15}$ (6), and $\text{K}_3\text{Ti}_8\text{O}_{17}$ (7). Other representatives of this class have tunnel structures, e.g., related to the hollandite structure as in $\text{A}_x\text{Ti}_8\text{O}_{16}$ ($A = \text{K}, \text{Rb}, \text{Cs}$) (8), or the calcium ferrite structure as in NaTi_2O_4 (9). Recently, more complicated tunnel structures have been observed in the reduced Na–Ti–O compounds $\text{Na}_2\text{Ti}_4\text{O}_9$ (10), and $\text{Na}_{1.7}\text{Ti}_6\text{O}_{11}$ (11). While investigating the use of borate fluxes for the crystallization of reduced ternary transition metal oxides under inert atmosphere we attempted recrystallization of the Ti^{3+} perovskites $\text{SrTiO}_{2.5}$ and LaTiO_3

from $\text{SrO} \cdot 2\text{B}_2\text{O}_3$ and $\text{La}_2\text{O}_3 \cdot 3\text{B}_2\text{O}_3$, respectively. It was observed that these fluxes can buffer the amount of SrO or La_2O_3 in the solid phase that crystallizes, producing new reduced ternary phases with a lower SrO or La_2O_3 content than in the original ceramic precursors. We report the formation and crystal structure of two new reduced ternary titanates, $\text{SrTi}_{11}\text{O}_{20}$ and $\text{La}_{1.33}\text{Ti}_8\text{O}_{16}$.

Experimental

Sample Preparation

A mixture of $\text{SrTiO}_{2.5}$ and $\text{SrO} \cdot 2\text{B}_2\text{O}_3$ (in 1 : 2 molar ratio) was placed in a Mo-foil cup with a Mo-foil lid, and heated *in vacuo* (in a Centorr high-vacuum furnace) to 400°C to remove adsorbed water, and then to 1100°C (1 hr, 10^{-6} – 10^{-7} Torr), after which the mixture was slowly cooled ($6^\circ\text{C}/\text{hr}$) to 940°C . The heater was subsequently turned off, allowing the sample to reach room temperature in 1 hr. The flux was removed using a dilute aqueous HF solution. The product

contained small purple crystals of up to 0.5 mm of $\text{SrTi}_{11}\text{O}_{20}$ (as determined by single crystal X-ray diffraction), together with very thin blue needles of an as yet unidentified species (also with low Sr-content, as indicated by EDAX).

A mixture of LaTiO_3 and $\text{La}_2\text{O}_3 \cdot 3\text{B}_2\text{O}_3$ (in 3 : 2 molar ratio) was similarly heated to 1250°C and cooled (6°C/hr) to 1140°C. The product proved moisture-sensitive, and the mixture had to be broken up mechanically. The reaction resulted in a solidified melt on top of which a layer of greenish-blue crystalline material had formed. Dark needles of a new lanthanum titanate, $\text{La}_{1.33}\text{Ti}_8\text{O}_{16}$ (as determined by single crystal X-ray diffraction), extended from this layer. Additionally, flattened crystals of Ti_2O_3 were present.

So far, attempts to prepare these new phases as ceramics (mixing SrO or La_2O_3 with Ti_2O_3 and TiO_2 in the correct stoichiometry, with some borate mineralizer added, and heating the mixtures *in vacuo* at 1100–1150°C for 24 hr) have been unsuccessful. Recrystallization of the ceramic with nominal composition " $\text{La}_{1.33}\text{Ti}_8\text{O}_{16}$ " from a $\text{K}_2\text{B}_4\text{O}_7$ flux in purified Ar atmosphere (cooling from 1000 to 800°C at 15°C/hr) yielded well-formed needles of the tetragonal potassium hollandite $\text{K}_{1.28}\text{Ti}_8\text{O}_{16}$ (as determined by EDAX and unit cell data from single crystal diffraction).

Ceramic $\text{SrTiO}_{2.5}$ and LaTiO_3 were synthesized by heating pressed pellets of SrO or La_2O_3 and Ti_2O_3 in the appropriate stoichiometry, together with 3–5 mole% of B_2O_3 as a mineralizer, wrapped in Mo-foil *in vacuo* to 1100°C for 24 hr. The Sr–Ti perovskite thus synthesized was cubic ($a = 3.9058(1)$ Å). TGA in oxygen resulted in a slightly higher weight gain than calculated for pure $\text{SrTiO}_{2.5}$, due to some leaching of SrO by the mineralizer: the X-ray powder pattern of the oxidized product showed some TiO_2 impurity. The borate $\text{SrO} \cdot 2\text{B}_2\text{O}_3$ was prepared by heating SrO_2 and B_2O_3 in a

TABLE I
CRYSTALLOGRAPHIC AND EXPERIMENTAL DATA

Formula	$\text{SrTi}_{11}\text{O}_{20}$	$\text{La}_{1.33}\text{Ti}_8\text{O}_{16}$
Space group	$P\bar{1}$	$I2/m$
Crystal size (mm)	$0.17 \times 0.11 \times 0.05$	$0.14 \times 0.04 \times 0.04$
a (Å) (at 25°C)	7.1252(8)	9.946(2)
b (Å)	7.6644(8)	2.9668(4)
c (Å)	13.157(2)	10.280(2)
α (°)	90.21(1)	
β (°)	92.79(1)	91.09(2)
γ (°)	103.94(1)	
V (Å ³)	696.4(2)	303.3(1)
Z	2	1
D_c (g/cm ³)	4.456	4.516
μ (MoK α , cm ⁻¹)	51.8	91.8
Scan type	ω	ω
Reflections measured	5461	1985
Independent reflections	4047	504
Observed reflections ($I > 2.5\sigma(I)$)	2400	448
Refined parameters	190	43
R	0.065	0.037
R_w ($w = 1/\sigma^2(F_0)$)	0.073	0.052

1 : 2 ratio to 900°C for 24 hr in an alumina crucible, and $\text{La}_2\text{O}_3 \cdot 3\text{B}_2\text{O}_3$ was prepared analogously from $\text{La}(\text{OH})_3$ and B_2O_3 in a 2 : 3 ratio.

Structure Determinations

The crystals were measured at 23°C on an Enraf–Nonius CAD-4 diffractometer using graphite-monochromatized MoK α radiation and the NRCCAD program package (12). All calculations were carried out on an Alliant FX/80 computer, using the NRCVAX structure package (13). Lattice parameters were determined from the absolute 2θ values of reflections at high angle ($\text{SrTi}_{11}\text{O}_{20}$: 36 reflections with $40^\circ < 2\theta < 50^\circ$, $\text{La}_{1.33}\text{Ti}_8\text{O}_{16}$: 20 reflections with $41^\circ < 2\theta < 52^\circ$). The metal atom positions were obtained by direct methods. A Gaussian absorption correction was applied, and anisotropic temperature factors for the metal atoms (and oxygen atoms in $\text{La}_{1.33}\text{Ti}_8\text{O}_{16}$) were included in the refinement. Further experimental and crystallographic data are listed in Table I, atomic coordinates and isotropic thermal parameters in Tables II and III.

TABLE II
ATOMIC POSITIONAL PARAMETERS AND ISOTROPIC
TEMPERATURE FACTORS FOR $\text{SrTi}_{11}\text{O}_{20}$

	<i>x</i>	<i>y</i>	<i>z</i>	$B_{\text{iso}}(\text{\AA}^2)$
Sr	0.53721(21)	0.18786(20)	0.23932(11)	0.84(4)
Ti(1)	0.0071(3)	0.9301(3)	0.20508(18)	0.37(7)
Ti(2)	0.6670(3)	0.5688(3)	0.07131(18)	0.33(7)
Ti(3)	0.9664(4)	0.5697(3)	0.29135(18)	0.50(8)
Ti(4)	0.6776(4)	0.4218(3)	0.48722(18)	0.37(7)
Ti(5)	0.3159(3)	0.0760(3)	0.00177(18)	0.38(7)
Ti(6)	0.6966(4)	0.7978(3)	0.41610(19)	0.50(8)
Ti(7)	0.3552(4)	0.6355(3)	0.28647(18)	0.45(8)
Ti(8)	0.3185(4)	0.9321(3)	0.43617(19)	0.42(8)
Ti(9)	0.3156(3)	0.7101(3)	0.08457(18)	0.41(8)
Ti(10)	0.0064(3)	0.2943(3)	0.12667(18)	0.39(8)
Ti(11)	0.0170(3)	0.2094(3)	0.36817(18)	0.38(8)
O(1)	0.8766(14)	0.1189(13)	0.2333(7)	0.42(13)
O(2)	0.1565(14)	0.7380(13)	0.2016(7)	0.39(13)
O(3)	0.8320(14)	0.1739(13)	0.0233(8)	0.59(14)
O(4)	0.8339(14)	0.8199(13)	0.0960(7)	0.49(14)
O(5)	0.1731(14)	0.4659(13)	0.0472(8)	0.61(14)
O(6)	0.8265(14)	0.3767(13)	0.3735(7)	0.43(14)
O(7)	0.4959(14)	0.8783(13)	0.3313(7)	0.45(14)
O(8)	0.1756(14)	0.1153(13)	0.1239(7)	0.50(14)
O(9)	0.4969(15)	0.1762(13)	0.4691(8)	0.59(14)
O(10)	0.1747(15)	0.3264(14)	0.4795(8)	0.65(15)
O(11)	0.1773(14)	0.6688(13)	0.4034(8)	0.52(14)
O(12)	0.8488(15)	0.7656(14)	0.3046(8)	0.63(14)
O(13)	0.8355(14)	0.0475(13)	0.4456(7)	0.44(14)
O(14)	0.8345(13)	0.4468(12)	0.1671(7)	0.31(13)
O(15)	0.4843(14)	0.9521(13)	0.0955(7)	0.45(14)
O(16)	0.1485(14)	0.4018(13)	0.2677(7)	0.52(14)
O(17)	0.1756(14)	0.0449(13)	0.3326(7)	0.51(14)
O(18)	0.4947(16)	0.5936(14)	0.1732(8)	0.88(16)
O(19)	0.5014(14)	0.3178(13)	0.0302(7)	0.43(13)
O(20)	0.5083(15)	0.5481(14)	0.3989(8)	0.72(15)

TABLE III
ATOMIC POSITIONAL PARAMETERS AND ISOTROPIC
TEMPERATURE FACTORS FOR $\text{La}_{1.33}\text{Ti}_8\text{O}_{16}$

	Occ.	<i>x</i>	<i>y</i>	<i>z</i>	$B_{\text{iso}}(\text{\AA}^2)$
La	0.334(3)	0.0	0.1531(7)	0.0	1.68(6)
Ti(1)		0.66880(13)	0.0	0.14655(12)	0.70(5)
Ti(2)		0.34734(13)	0.5	0.16409(13)	0.68(5)
O(1)		0.3192(5)	0.0	0.0395(5)	0.87(20)
O(2)		0.1507(5)	0.5	0.2034(5)	0.69(18)
O(3)		0.8047(5)	0.5	0.1593(5)	0.67(19)
O(4)		0.5395(5)	0.5	0.1545(5)	0.86(19)

chains (14) of edge-sharing TiO_6 -octahedra running along the [010] direction that are sheared after every block of six octahedra. The A layer is shown separately, viewed approximately along the *a*-axis, in Fig. 2a. The first octahedron of each individual block shares one edge with each of the two last octahedra of the previous block, forming a double zig-zag chain. There are two crystallographically independent double

Description of the Structures

$\text{SrTi}_{11}\text{O}_{20}$

The compound $\text{SrTi}_{11}\text{O}_{20}$ crystallizes in the triclinic space group $P\bar{1}$, and its unit cell contains eleven crystallographically independent octahedrally coordinated Ti-atoms. A polyhedral representation of the crystal structure is shown in Fig. 1, viewed along the *b*-axis. Selected interatomic distances are listed in Table IV. The structure can be considered as being built from two types of layers of TiO_6 -octahedra parallel to [100], connected by oxygen sharing. One layer (A in Fig. 1) consists of parallel "double rutile"

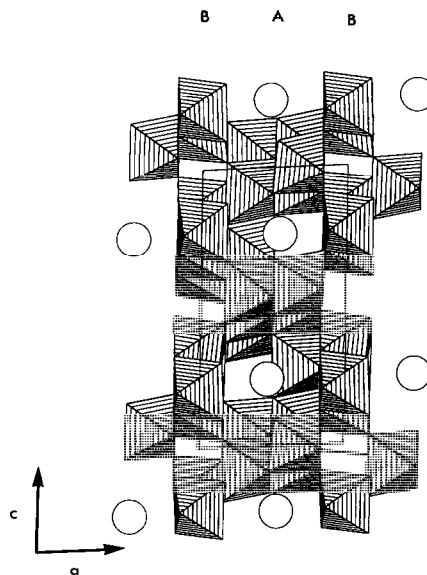


FIG. 1. Polyhedral representation of the structure of $\text{SrTi}_{11}\text{O}_{20}$, viewed along the *b*-axis. Sr-atoms are represented by circles.

TABLE IV

SELECTED INTERATOMIC DISTANCES (Å) FOR $\text{SrTi}_{11}\text{O}_{20}$, WITH ESTIMATED STANDARD DEVIATIONS IN PARENTHESES

Sr-O(1)	2.60(1)	Ti(6)-O(7)	1.99(1)
-O(6)	2.766(9)	-O(9)	2.13(1)
-O(7)	2.63(1)	-O(10)	1.99(1)
-O(8)	2.86(1)	-O(12)	1.92(1)
-O(14)	2.741(9)	-O(13)	1.96(1)
-O(15)	2.56(1)	-O(20)	2.06(1)
-O(17)	2.88(1)	Ti(7)-O(2)	2.06(1)
-O(19)	2.95(1)	-O(7)	1.96(1)
Ti(1)-O(1)	1.94(1)	-O(11)	2.09(1)
-O(2)	2.02(1)	-O(16)	2.03(1)
-O(4)	1.90(1)	-O(18)	1.90(1)
-O(8)	1.98(1)	-O(20)	2.01(1)
-O(12)	2.01(1)	Ti(8)-O(7)	2.02(1)
-O(17)	2.08(1)	-O(9)	2.02(1)
Ti(2)-O(4)	2.02(1)	-O(11)	2.08(1)
-O(5)	2.03(1)	-O(13)	2.06(1)
-O(14)	2.07(1)	-O(17)	1.97(1)
-O(18)	1.90(1)	-O(17)	1.98(1)
-O(19)	2.05(1)	Ti(9)-O(2)	2.00(1)
	2.08(1)	-O(3)	2.06(1)
Ti(3)-O(2)	2.05(1)	-O(5)	1.95(1)
-O(6)	1.94(1)	-O(15)	1.95(1)
-O(11)	2.06(1)	-O(18)	2.05(1)
-O(12)	1.90(1)	-O(19)	2.09(1)
-O(14)	1.964(9)	-O(1)	2.04(1)
-O(16)	2.07(1)	-O(3)	1.88(1)
Ti(4)-O(6)	1.95(1)	-O(5)	1.90(1)
-O(9)	2.01(1)	-O(8)	2.03(1)
-O(10)	2.00(1)	-O(14)	1.97(1)
-O(11)	1.96(1)	-O(16)	2.13(1)
-O(20)	2.04(1)	Ti(11)-O(1)	2.03(1)
	2.09(1)	-O(6)	2.08(1)
Ti(5)-O(3)	1.97(1)	-O(10)	1.89(1)
-O(4)	1.93(1)	-O(13)	1.90(1)
-O(8)	1.99(1)	-O(16)	2.07(1)
-O(15)	2.07(1)	-O(17)	1.95(1)
	2.01(1)		
-O(19)	2.02(1)		

chains in the structure (around $z = 0$, Ti(2, 5, 9), and $z = 1/2$, Ti(4, 6, 8), respectively), and they are interconnected by a single TiO_6 -octahedron (Ti(7)). This caps three octahedra of the $z = 1/2$ chain by sharing three edges, while sharing only one edge with one octahedron in the $z = 0$ chain. In this way a 2D-network is formed with cavities for the

Sr-atoms. The B layer (shown in Fig. 2b) consists of parallel single chains of edge-sharing TiO_6 -octahedra (Ti(1, 3, 10, 11)) that are sheared after every block of four octahedra. The first two octahedra of a block share edges with the two last octahedra of the previous block. These chains also run parallel to the b -axis and are centered around $z = 1/4, 3/4$, thus "capping" the Sr-containing cavities in the A layer.

An alternative description of the structure is based on the presence of close-packed layers of ions parallel to [100]. Around $x = 1/6, 5/6$ oxygen atoms form a close-packed layer (Y), while around $x = 1/2$ the O and Sr ions form a distorted SrO_6 layer (Z). The layer stacking sequence is $[\text{YYZ}]_\infty$, and the A layer of octahedra is associated with ordering of Ti-ions in octahedral holes in the YZY sequence, the B layer of octahedra with ordering of Ti-ions in octahedral holes in the YY sequence.

The Sr-ion occupies a somewhat distorted cuboctahedral site that appears to be too large for a regular 12-coordination of the cation. The average Sr-O distance is 2.95 Å, significantly larger than, e.g., the 2.76 Å for cuboctahedral Sr in SrTiO_3 (15). The Sr-ion is clearly positioned off-center in the site, and three of the Sr-O distances exceed 3.3 Å. The average of the remaining nine Sr-O distances is 2.78 Å.

As is to be expected in structures composed of multiply edge-sharing octahedra, the TiO_6 -octahedra in $\text{SrTi}_{11}\text{O}_{20}$ are all more or less distorted due to the mutual repulsion of the Ti-ions. All diagonal O-Ti-O angles are smaller than 175° (180° for an undistorted octahedron), and for three of the four Ti-atoms in the B layer (Ti(3, 10, 11)) even smaller than 170° . The strongest distortion is exhibited by Ti(10), with O-Ti-O diagonal angles of 168.2° , 165.8° , and 164.7° , and Ti-O distances ranging from 1.88 to 2.13 Å.

In the ionic limit, the compound can be formulated by charge compensation as $\text{Sr}^{2+}\text{Ti}_6^{3+}\text{Ti}_5^{4+}\text{O}_{20}^{2-}$, giving an average Ti oxi-

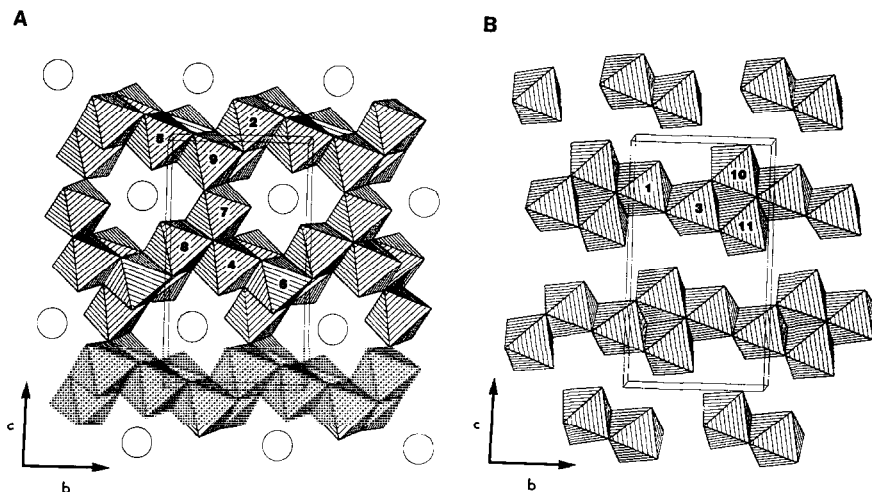


FIG. 2. (a) Layer A in the structure of $\text{SrTi}_{11}\text{O}_{20}$, viewed approximately along the a -axis; (b) layer B of the structure, viewed along the same direction as (a). The TiO_6 octahedra are labeled with the number of the Ti-atom in the center of the octahedron.

ation state of $3.45+$. The average Ti–O distance is 2.006 \AA , which lies between the values generally observed for compounds containing only Ti^{4+} (1.97 \AA , as, e.g., in TiO_2 (16)), or Ti^{3+} (2.05 \AA , as in Ti_2O_3 (17)). The average Ti–O distances for the TiO_6 -octahedra in the A layer (overall 2.014 \AA) are all slightly larger than for those in the B-layer (overall 1.992 \AA), but this difference is on the borderline of significance, and does not allow any conclusions with respect to possible site preference for either Ti^{3+} or Ti^{4+} in the structure.

Attempts to perform single-crystal resistivity measurements on $\text{SrTi}_{11}\text{O}_{20}$ have failed so far due to the high contact resistance of Ag/epoxy or evaporated silver contacts on the crystal surface as obtained after etching away the flux, and the small size of the crystals, which precludes cleavage to obtain a fresh contact surface.

$\text{La}_{1.33}\text{Ti}_8\text{O}_{16}$

This phase crystallizes in the hollandite-type tunnel structure, which is slightly mo-

noclinically distorted for the La-compound ($\text{K}_{1.35}\text{Ti}_8\text{O}_{16}$, the other known reduced Ti-hollandite, is tetragonal $I4/m$, $a = 10.188(2) \text{ \AA}$, $c = 2.9661(7) \text{ \AA}$ (18)). Although rarely observed for Ti-hollandites, monoclinic deformation of hollandite-type oxides occurs quite commonly, e.g., in the minerals cryptomelane and hollandite itself (19). This appears to be related to the ratio r_B/r_A of the ionic radii for the octahedrally coordinated cations and the tunnel site cations, respectively. Monoclinic distortion is generally observed for $r_B/r_A > 0.48$ (19), and the value of 0.64 for $\text{La}_{1.33}\text{Ti}_8\text{O}_{16}$ easily meets this requirement.

The structure of $\text{La}_{1.33}\text{Ti}_8\text{O}_{16}$ is shown in Fig. 3, projected along the b -axis. Selected interatomic distances are listed in Table V. The hollandite structure is based on linear "double rutile" chains of edge-sharing TiO_6 -octahedra that run parallel to the unique axis, and are linked together to form a framework of parallel tunnels. The A-cation resides in the tunnel, and ordering and correlation of occupied and vacant sites often form commensurate or incommensurate

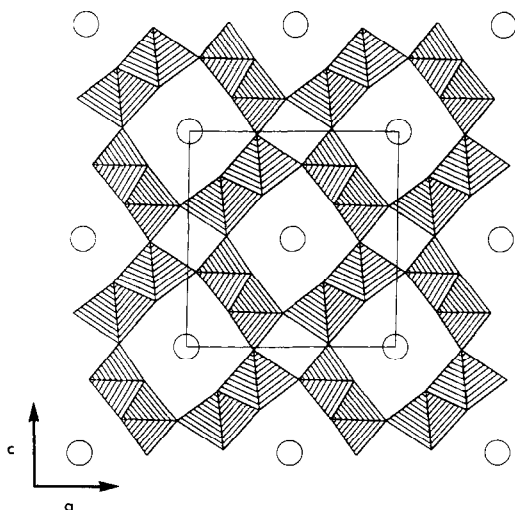


FIG. 3. Polyhedral representation of the structure of $\text{La}_{0.33}\text{Ti}_2\text{O}_4$, viewed along the b -axis. The La-atom positions, represented by circles, are partially occupied.

superstructures. This phenomenon has been extensively studied, e.g., by X-ray and electron diffraction (see for example (20) and references cited therein). As observed in other hollandite-type oxides with a relatively small cation occupying the tunnel sites (19), the La-ion in $\text{La}_{1.33}\text{Ti}_8\text{O}_{16}$ is displaced from the special position along the tunnel direction and thus occupies an acen-

tric position in the distorted cuboctahedral site. Although the ordering of the La-ions in $\text{La}_{1.33}\text{Ti}_8\text{O}_{16}$ has not been explicitly investigated, the presence of some weak superlattice reflections with indices $(h, k + 2/3, l)$ suggest a commensurate or near-commensurate tripling of the b -axis.

An interesting feature of $\text{La}_{1.33}\text{Ti}_8\text{O}_{16}$ is that it appears to be the first hollandite with a trivalent cation occupying the tunnel sites. As its stoichiometry is similar to that of the well-known $\text{K}_{1.35}\text{Ti}_8\text{O}_{16}$, it implies that $\text{La}_{1.33}\text{Ti}_8\text{O}_{16}$ is much more reduced than other reduced Ti-hollandites (although recently some strongly reduced hollandites with the general formula $\text{Li}_x\text{Ti}_2\text{MTi}_7\text{O}_{16}$ ($M = \text{Al, Fe, Mg, Ni; } x < 6$) have been prepared by Li-intercalation (21)). In the ionic limit, it can be formulated as $\text{La}_{1.33}^{3+}\text{Ti}_4^{4+}\text{O}_{16}^{2-}$, corresponding to an average Ti oxidation state of 3.5+. The average Ti-O distance in $\text{La}_{1.33}\text{Ti}_8\text{O}_{16}$ of 1.983 Å is somewhat longer than in $\text{K}_{1.35}\text{Ti}_8\text{O}_{16}$ (1.975 Å).

As it proved difficult to prepare $\text{La}_{1.33}\text{Ti}_8\text{O}_{16}$ crystals in quantity or as a ceramic, an attempt was made to recrystallize a ceramic with a corresponding nominal composition from a borate flux with a lower melting point, $\text{K}_2\text{B}_4\text{O}_7$ (mp 815°C). This resulted, however, in partial oxidation and formation of a large quantity of deep blue needles of the tetragonal potassium titanate hollandite $\text{K}_x\text{Ti}_8\text{O}_{16}$ (cell parameters from single crystal X-ray diffraction: $a = 10.170(1)$ Å; $c = 2.9649(2)$ Å; $x = 1.28(2)$, from semiquantitative EDAX).

TABLE V

SELECTED INTERATOMIC DISTANCES (Å) FOR $\text{La}_{1.33}\text{Ti}_8\text{O}_{16}$, WITH ESTIMATED STANDARD DEVIATIONS IN PARENTHESES

Ti(1)-O(1)	1.919(5)	Ti(2)-O(1)	1.976(3)	2×
-O(3)	2.010(3)	-O(2)	2.005(5)	
	2.008(5)		2.014(3)	2×
-O(4)	1.966(4)	-O(4)	1.916(5)	
La-O(1)	3.225(5)			
-O(2)	2.749(5)			
	3.202(4)			
-O(3)	2.763(5)			
	3.214(4)			
-O(4)	3.609(5)			

Conclusions

As we observed previously in the crystallization of reduced ternary niobate species (22-24), borate fluxes are useful media for obtaining single crystals of reduced ternary transition metal oxides. It appears, however, that reduced titanates are considerably more susceptible to partial oxidation

through oxygen or water gettering than reduced niobates, even under high-vacuum conditions. In this case, starting from Ti^{3+} ceramics, it has led to the formation of new mixed-valence phases. The buffering ability of the borate fluxes for alkaline-earth or lanthanide oxides allows formation of solid phases with metal ratios different from the starting material. Here the products are considerably depleted in SrO and La_2O_3 , respectively, relative to the starting material (borates can also act as an oxide source, e.g., in the reaction between NbO_2 and $BaO \cdot 3B_2O_3$ (22, 24)).

As it has been impossible so far to prepare the new phases separately by ceramic procedures, it may well be that the flux plays a very important role in the thermodynamics of the product formation. In the reduced Sr–Ti–O phase diagram (studied on ceramics at 1350°C), Roy *et al.* observed a Sr-poor phase, tentatively identified as $SrTi_{12}O_{19}$ (25). It is likely that this phase is not related to $SrTi_{11}O_{20}$, as the reported X-ray powder diffraction pattern for “ $SrTi_{12}O_{19}$ ” and the calculated pattern for $SrTi_{11}O_{20}$ are very different. The reaction between reduced ternary transition metal oxides and borate fluxes provides an interesting means to obtain new reduced ternary phases.

Acknowledgment

B.H. thanks the Netherlands Organization for Scientific Research (NWO) for the award of a fellowship.

References

1. J. F. SCHOOLEY, W. R. HOSLER, AND M. L. COHEN, *Phys. Rev. Lett.* **12**, 474 (1964).
2. C. S. KOONCE, M. L. COHEN, J. F. SCHOOLEY, W. R. HOSLER, AND E. R. PFEIFFER, *Phys. Rev.* **163**, 163 (1967).
3. M. R. HARRISON, P. P. EDWARDS, AND J. B. GOODENOUGH, *Phil. Mag.* **52**, 679 (1985).
4. M. ITOH, Y. HASEGAWA, H. YASUOKA, Y. UEDA, AND K. KOSUGE, *Physica* **157**, 65 (1989).
5. S. ANDERSSON AND A. D. WADSLEY, *Acta Crystallogr.* **14**, 1245 (1961).
6. A. D. WADSLEY AND W. G. MUMME, *Acta Crystallogr. Sect. B* **24**, 392 (1968).
7. J. A. WATTS, *J. Solid State Chem.* **1**, 319 (1970).
8. G. BAYER AND W. HOFFMAN, *Am. Miner.* **51**, 511 (1966).
9. J. AKIMOTO AND H. TAKEI, *J. Solid State Chem.* **79**, 212 (1989).
10. J. AKIMOTO AND H. TAKEI, *J. Solid State Chem.* **83**, 132 (1989).
11. J. AKIMOTO AND H. TAKEI, *J. Solid State Chem.* **85**, 8 (1990).
12. Y. LEPAGE, P. S. WHITE, AND E. J. GABE, “Proceedings of the American Crystallographic Association Annual Meeting, 1986; Hamilton, Canada;” AIP, New York, (1986). [Poster PA23]
13. E. J. GABE, Y. LEPAGE, J. P. CHARLAND, F. L. LEE, AND P. S. WHITE, *J. Appl. Crystallogr.* **22**, 384 (1989).
14. A. F. WELLS, “Structural Inorganic Chemistry,” 5th ed., p. 214, Clarendon, Oxford (1984).
15. Calculated from the cell parameter for $SrTiO_3$ ($a = 3.905 \text{ \AA}$) and the geometry of the ideal perovskite structure.
16. S. C. ABRAHAMS AND J. L. BERNSTEIN, *J. Chem. Phys.* **55**, 3206 (1971).
17. C. T. PREWITT, R. D. SHANNON, D. B. ROGERS, AND A. W. SLEIGHT, *Inorg. Chem.* **8**, 1985 (1969).
18. T. VOGT, E. SCHWEDA, C. WUESTEFELD, J. STRAEHLE, AND A. K. CHEETHAM, *J. Solid State Chem.* **83**, 61 (1989).
19. J. E. POST, R. B. VON DREELE, AND P. R. BUSECK, *Acta Crystallogr. Sect. B* **38**, 1056 (1982).
20. H. U. BEYELER AND C. SCHUELER, *Solid State Ionics* **1**, 77 (1980).
21. E. WANG, J. M. TARASCON, S. COLSON, AND M. TSAI, *J. Electrochem. Soc.* **138**, 166 (1991).
22. S. A. SUNSHINE, B. HESSEN, T. SIEGRIST, A. T. FIORY, AND J. V. WASZCZAK, in “Chemistry of Electronic Ceramic Materials” (P. K. Davies, R. S. Roth, Eds.), Natl. Inst. Stand. Technol. Special Publication 804, p. 237 (1991).
23. B. HESSEN, S. A. SUNSHINE, T. SIEGRIST, AND R. JIMENEZ, *Mater. Res. Bull.* **26**, 85 (1991).
24. B. HESSEN, S. A. SUNSHINE, T. SIEGRIST, A. T. FIORY, AND J. V. WASZCZAK, *Chem. Mater.*, **3**, 528 (1991).
25. G. J. MCCARTHY, W. B. WHITE, AND R. ROY, *J. Am. Ceram. Soc.* **52**, 463 (1969).